

RESEARCH ARTICLE

Comparative characterization of SARS-CoV-2 variants of concern and mouse-adapted strains in mice

Qi Chen¹ | Xing-Yao Huang¹ | Yu Liu¹ | Meng-Xu Sun¹ | Bin Ji² |
Chao Zhou¹ | Hang Chi¹ | Rong-Rong Zhang¹ | Dan Luo¹ | Ying Tian¹ |
Xiao-Feng Li¹ | Hui Zhao¹ | Cheng-Feng Qin^{1,3} 

¹State Key Laboratory of Pathogen and Biosecurity, Department of Virology, Beijing Institute of Microbiology and Epidemiology, AMMS, Beijing, China

²Department of Disease Control, Wuxi Center for Disease Control and Prevention, Wuxi, Jiangsu Province, China

³Research Unit of Discovery and Tracing of Natural Focus Diseases, Chinese Academy of Medical Sciences, Beijing, China

Correspondence

Cheng-Feng Qin, State Key Laboratory of Pathogen and Biosecurity, Department of Virology, Beijing Institute of Microbiology and Epidemiology, AMMS, 100071 Beijing, China.
Email: qincf@bmi.ac.cn

Funding information

National Key Research and Development Projects of the Ministry of Science and Technology of China (2021YFC2301300); National Key Research and Development Project of China (2020YFC0842200, 2020YFA0707801, and 2021YFC0863300); National Natural Science Foundation of China (No. 82041044)

Abstract

SARS-CoV-2 has evolved into a panel of variants of concern (VOCs) and constituted a sustained threat to global health. The wildtype (WT) SARS-CoV-2 isolates fail to infect mice, while the Beta variant, one of the VOCs, has acquired the capability to infect standard laboratory mice, raising a spreading risk of SARS-CoV-2 from humans to mice. However, the infectivity and pathogenicity of other VOCs in mice remain not fully understood. In this study, we systematically investigated the infectivity and pathogenicity of three VOCs, Alpha, Beta, and Delta, in mice in comparison with two well-understood SARS-CoV-2 mouse-adapted strains, MASCP6 and MASCP36, sharing key mutations in the receptor-binding domain (RBD) with Alpha or Beta, respectively. Our results showed that the Beta variant had the strongest infectivity and pathogenicity among the three VOCs, while the Delta variant only caused limited replication and mild pathogenic changes in the mouse lung, which is much weaker than what the Alpha variant did. Meanwhile, Alpha showed comparable infectivity in lungs in comparison with MASCP6, and Beta only showed slightly lower infectivity in lungs when compared with MASCP36. These results indicated that all three VOCs have acquired the capability to infect mice, highlighting the ongoing spillover risk of SARS-CoV-2 from humans to mice during the continued evolution of SARS-CoV-2, and that the key amino acid mutations in the RBD of mouse-adapted strains may be referenced as an early-warning indicator for predicting the spillover risk of newly emerging SARS-CoV-2 variants.

KEYWORDS

cytokine assay, lung pathology, mice, mouse-adapted strains, SARS-CoV-2, spillover risk, variants of concern

1 | INTRODUCTION

As the COVID-19 pandemic continues, its causative agent, the SARS-CoV-2, keeps progressing in human populations. During the process, mutations in the genome gradually appear and

accumulate, which have led to several variants of concern (VOC), mainly including the variants Alpha, Beta, Gamma, and Delta.^{1,2}

The variant Alpha was firstly isolated in England in September 2020, and then rapidly became the dominant variant in the United Kingdom and spread to more than 190 countries or regions around

the world, featured with seven substitutions and three deletions in Spike (S) protein, including N501Y in the receptor-binding domain (RBD).³ Following the appearance of Alpha, the variant Beta was announced in South Africa in December 2020 and then detected in more than 140 countries within a few months, characterized by eight mutations in S protein, including K417N, E484K, and N501Y in RBD.⁴ Among the co-circulating strains, the proportion of these two variants peaked in February to April 2021, at which the variant Delta began to appear in India, featured with E484Q and L452R mutations in S protein.^{1,5} In a short period, the variant Delta spread quickly across the globe and became the most dominant strain worldwide.⁶

These mutations that occurred in the RBD of SARS-CoV-2 S protein are especially concerning, as the RBD is responsible for inducing neutralizing antibodies and mediating virus entry into host cells. The WT SARS-CoV-2 cannot effectively infect laboratory standard mice, because its RBD has a low binding affinity to mACE2.^{7,8} However, we recently found that the Beta variant has acquired the capability to infect laboratory standard mice, which is mainly caused by the mutations in the RBD, reminding us of the spreading risk of SARS-CoV-2 from humans to mice.⁵ What's worse, some preliminary results from biochemical assay and pseudoviruses indicate that the RBD of other VOCs, even including those sharing no mutations with the RBD of Beta variant, also showed increased binding affinity to mACE2,⁹⁻¹³ indicating it is necessary to further confirm whether these VOCs are also capable of infecting mice and causing spillover risk.

Herein, in this study, we sought to determine the infectivity and pathogenicity of three major VOCs, Alpha, Beta, and Delta, in mice. In previous studies, we and others developed several SARS-CoV-2 mouse-adapted strains by serially passaging of prototype SARS-CoV-2 strains in mice, which can effectively infect mice and cause pathological changes.^{9,14-19} The mouse infectivity of these mouse-adapted strains has been demonstrated to be largely related to the amino acid mutations identified in the RBD. By alignment, we found that among all the reported mouse-adapted strains, only MASCP6 and MASCP36 share key mutations in S protein with Alpha or Beta, respectively. Thus, in this study, we chose these two mouse-adapted strains as references for evaluating the infectivity and pathogenicity of VOCs.

2 | MATERIALS AND METHODS

2.1 | Ethics approval and consent to participate

All procedures involving infectious virus were conducted in the biosafety level 3 (BSL-3) laboratory at the Beijing Institute of Microbiology and Epidemiology, AMMS, and were approved by the Animal Experiment Committee of the Laboratory Animal Center, Beijing Institute of Microbiology and Epidemiology (approval code number: IACUC-IME-2021-023).

2.2 | Mouse and virus

Nine-month-old female BALB/c mice were from Beijing Vital River Laboratory Animal Technology Co., Ltd. The SARS-CoV-2 strain BetaCov/human/CHN/Beijing_IME-BJ05/2020 (IME-BJ05, accession no. GWHACAX01000000) was used as the WT SARS-CoV-2 in this study.⁵ The Alpha variant (C-Tan-BJ202101) was from the Chinese Center for Disease Control and Prevention. The Beta variant (GDPC, CSTR: 16698.06.NPRC2.062100001) was from the National Pathogen Resource Center.²⁰ The Delta variant (CCPM-B-V-049-2105-8) was from the Chinese Academy of Medical Sciences. The mouse-adapted strains MASCP6 and MASCP36 were generated by serial passaging in our previous studies.^{9,14} These viruses were titrated by a standard plaque assay in Vero cells.

2.3 | Mouse experimental designs

Mice were first anesthetized with sodium pentobarbital at a dose of 50 mg/kg through the intraperitoneal route, and then intranasally infected with 2.4×10^3 PFU of each SARS-CoV-2 strain ($n = 9$) or the same volume of Phosphate Buffered Saline (PBS) (mock, $n = 3$). Three mice in each group were then killed on Days 1-3 post-infection for tissue processing.

2.4 | Measurement of viral sgRNA

Lung and tracheahomogenates were centrifuged at 6000 rpm for 6 min for supernatant collection. Viral RNA in the supernatants was extracted using the QIAamp Viral RNA Mini Kit (Qiagen) according to the manufacturer's protocol. sgRNA in each sample was quantified by reverse transcription-quantitative real-time PCR (RT-qPCR) (using One Step PrimeScript RT-PCR Kit (Takara) with the following primers and probes targeting the S gene of SARS-CoV-2: sgRNA-F (5'- C GATCTCTGTAGATCTGTTCTC-3'); sgRNA-R (5'- ATATTGCAGCAG TACGCACACA-3'); and sgRNA-P3 (5'- AACTAGCCATCCTTACT GCGCTTCG-3').

2.5 | RNA ISH assay

Lung tissues were fixed in 4% paraformaldehyde for 48 h, and then made into 4 μ m of paraffin-embedded tissue sections in accordance with the standard procedure. The tissue sections were deparaffinized by incubation for 60 min at 60°C, and then the SARS-CoV-2 genome RNA ISH assay for tissue sections was performed with RNAscope2.5 HD Reagent Kit (Advanced Cell Diagnostics) according to the manufacturer's instruction. Simply, the endogenous peroxidases were quenched with hydrogen peroxide for 10 min at room temperature, and then the tissue sections were boiled for 15 min in RNAscope Target Retrieval Reagents and incubated for 30 min in RNAscope Protease Plus before probe hybridization. Tissues were

counterstained with Gill's hematoxylin and visualized with standard bright-field microscopy.⁵

2.6 | Immunofluorescence staining

For immunostaining, deparaffinized tissue sections were placed in ethylene diamine tetraacetic acid (pH 9.0) for 1 h at 96°C for antigen retrieval. The endogenous peroxidases were first inactivated with 3% hydrogen peroxide for 25 min, and then the sections were blocked with 3% bovine serum albumin for 30 min. SARS-CoV/SARS-CoV-2 Nucleocapsid (N) Antibody, Mouse Mab (Sino Biological, 1:500) was used as the primary antibody for incubating with the sections for 2 h in a humidified chamber at 37°C. After three washes, the sections were incubated with the fluorescein isothiocyanate-labeled secondary antibody (Zhongshan Biotechnology) for 1 h followed by 5 min of 4,6-diamino-2-phenyl indole staining.⁵

2.7 | Histopathological examination

The deparaffinized sections were stained with H&E and examined by light microscopy. The semiquantitative assessment was performed as follows.¹⁴ For the degree of degeneration of alveolar epithelial cells and bronchiolar epithelial cells, we scored 0 when no cell degeneration was observed, scored 1 when the cell degeneration was less than 10% and scored 2 when the degeneration was 10%–50%. For the degree of alveolar septal thickening, we scored 0 when no alveolar septal thickening was observed, scored 1 when the alveolar septal thickening area was less than 10%, scored 2 when the area was 10%–20%, scored 3 when the area was 20%–50%, scored 4 when the area was >50%, and a score of 1 was added when alveolar wall fusion area was less than 10%, a score of 2 was added when the area was 10%–20%, and a score of 3 was added when the area was 20%–50%, and a score of 4 was added when the area was >50%. For the degree of edema, we scored 0 when no edema was observed, scored 1 when occasional edema was visible, and scored 2 when the edema was seen for 10%–50% of vascular, scored 3 when the edema was seen for >50% of vascular. For the degree of inflammatory cells infiltration, we scored 0 when no inflammatory cell infiltration, scored 1 when occasional infiltration of a single inflammatory cell was visible and scored 2 when focal infiltration of inflammatory cells was visible. For the degree of hemorrhage, we scored 0 when no hemorrhage was observed, scored 1 when occasional hemorrhage was visible and scored 2 when focal hemorrhage was visible. For the degree of bronchial epithelial cell damage and bronchial obstruction, we scored 0 when no bronchial epithelial cell damage was observed, scored 1 when occasional bronchial epithelial cell damage was visible and scored 2 when the epithelial cell damage was seen for 10%–20% of bronchi, scored 3 when the epithelial cell damage was seen for 20%–50% of bronchi, scored 4 when the epithelial cell damage was seen for >50% of bronchi, and a score of 1 was added when the occasional bronchial obstruction was observed, a score of 2 was added when it was observed for 10%–20% of bronchi, a score of 3 was added

when it was seen for 20%–50% of bronchi. The lesion of the lung was observed by an experienced experimental pathologist who focuses on the pathogenesis study of virus infection, and the average of the three animals was taken as the total score for that group.

2.8 | Cytokine assay

Tissue homogenates were centrifuged at 6000 rpm for 6 min for supernatant collection. The supernatants were then inactivated at 56°C for 60 min. Twenty-five microliters inactivated supernatants from each mouse was adopted for cytokine analysis with Mouse Cytokine & Chemokine Panel 1A (36 plex) (Invitrogen) according to the manufacturer's instructions. The data were collected on Luminex 200 and analyzed by Luminex PONENT (Thermo Fisher).⁹

2.9 | Statistical analysis

Statistical analyses were carried out using Prism software (GraphPad Prism 7.0). Data of semiquantitative analysis of the H&E-stained lung sections are presented as mean. Other data are presented as mean ± SEM. Statistical details of experiments and animal replication numbers (*n*) are stated in the relevant figure legends and method details. Statistical significance among different groups was calculated using Student's *t*-test.

3 | RESULTS

3.1 | The shared mutations between VOCs and mouse-adapted strains

The S protein of the three VOCs was aligned with all the reported SARS-CoV-2 mouse-adapted strains.^{9,14–19} As shown in Figure 1, the only mutation N501Y in the RBD of Alpha is the same as that in mouse-adapted strain MASCP6. For the variant Beta, three mutations (K417N/E484K/N501Y) are found in the RBD. The K417N mutation is found in two of these mouse-adapted strains, CMA3p20 and MASCP36, and two of them (K417N/N501Y) are consistent with that in MASCP36 (K417N/Q493H/N501Y). Interestingly, no mutations outside of RBD within the S protein of Alpha and Beta are found in any mouse-adapted strains. For Delta, all amino acid mutations in the S protein, including the L452R and T478K in the RBD, are not found in any mouse-adapted strains. These results indicate that the mouse-adapted strains MASCP6 and MASCP36 are suitable to be referenced for evaluating the infectivity of Alpha and Beta, respectively.

3.2 | The BALB/c mice are susceptible to intranasal infection of all three VOCs

To investigate the mouse susceptibility to SARS-CoV-2 VOCs, 9-month-old female BABL/c mice were intranasally challenged

	NTD													RBD						SD1-2					S2											
	18	19	69	70	80	144	156	157	158	215	242	243	244	417	452	478	484	493	498	499	501	570	614	655	675	676	677	678	679	681	701	716	950	969	982	1118
WT	L	T	H	V	D	Y	E	F	R	D	L	A	L	K	L	T	E	Q	Q	P	N	A	D	H	Q	T	Q	T	N	P	A	T	D	N	S	D
Alpha	Y	D	G	H	.	I	.	.	A	H
Beta	F	.	.	.	A	G	.	.	.	N	.	.	K	.	.	.	Y	.	G	V	
Delta	.	R	G	R	K	G	R	.	.	N	.	.	.
MASCp6	Y
MASCp36	N	.	.	.	H	.	.	Y	
LG	Y
MA	Y	T
MA10	K	Y	T
HRB26M	H	S	.
CMA3p20	N	Y
C57MA14	H
QH-329-037	H

FIGURE 1 Schematic of amino acid mutations in the S protein of SARS-CoV-2 variants and mouse-adapted SARS-CoV-2 strains relative to the reference sequence. A dot indicates an identical amino acid at the indicated position, while a dash indicates an amino acid deletion at the indicated position. NTD, N-terminal domain; RBD, receptor-binding domain; SD, subdomain

with the same dose of WT, Alpha, Beta, and Delta variants, and MASCp6 or MASCp36 were used as control (Figure 2A). All animals were killed on Days 1–3 post-infection, and SARS-CoV-2 subgenomic RNA (sgRNA) quantitation was performed for detecting the viral replication in lung and trachea of infected mice (Figure 2A). As shown in Figure 2B, SARS-CoV-2 sgRNA can be detected in lung tissues from mice infected with all three variants, with Beta producing the highest level of viral sgRNA at all indicated time points. In comparison with Beta, Alpha produced relatively less sgRNA at all the three-time points. The least sgRNA was found in Delta-infected mice, which was comparable with that in Alpha-infected mice on Day 1 post-infection, but obviously less on Days 2 and 3 post-infection (Figure 2B). As expected, no sgRNA was detected in WT-infected mice. In comparison, the variant Alpha and MASCp6 produced comparable levels of sgRNA at all indicated time points, while the sgRNA in the lung of Beta reached a slightly lower peak than that of MASCp36. RNAScope in situ hybridization assay and immunofluorescence staining further confirmed the production of viral RNA (Figure 2C) and N protein (Figure 2D) in lung tissues of all three variants-infected mice.

In the trachea, both MASCp6 and MASCp36 produced detectable sgRNA (Figure 2E), while no detectable sgRNA was found in that of Alpha-infected mice, and only one out of the three mice produced detectable sgRNA in Delta-infected mice. Meanwhile, notably, a high level of sgRNA in the trachea of Beta-infected mice was detected, which even reached a higher peak than that in the trachea of MASCp36-infected mice on Day 2 post-infection (Figure 2E). These results demonstrate that all three VOCs acquired the infectivity for mice, with the Beta variant showing higher infectivity than Alpha and Delta variants. Meanwhile, on the whole, the mouse infectivity is comparable between the VOCs and mouse-adapted strains sharing key mutations in the RBD. However, notably, the specific infectivity rank of these VOCs and mouse-adapted strains in lungs (MASCp36 > Beta > MASCp6/Alpha > Delta) and trachea (Beta > MASCp36 >

MASCp6 > Delta/Alpha) (Figure 2F) is not completely consistent, indicating the tropism of these strains for the upper respiratory tract is not always positively associated with that for the lower respiratory tract.

3.3 | Pathological features induced by intranasal infection of VOCs in mice

To further characterize the pathological outcomes in mice infected with the VOCs, lung tissues collected on Day 3 post-infection from infected mice or mock (PBS) were subjected to histopathological investigation. Microscopic observation of H&E-stained lung sections showed mild pathological alterations in Delta-infected mice, characterized by local alveolar septal thickening and occasional congestion and edema around vessels (Figure 3A). In comparison, more obvious pathological damage, including more severe alveolar septal thickening and even alveolar structure collapsing, edema around vessels and activated inflammatory cell infiltration, was observed in Alpha and MASCp6-infected mice (Figure 3A). In addition, hemorrhage and damaged bronchial epithelial cells were further observed in Beta and MASCp36-infected mice (Figure 3A). More seriously, in MASCp36-infected mice, obvious bronchial obstruction by damaged bronchial epithelial cells and macrophages was observed (Figure 3A). Overall, by semiquantitative analysis and ranking, pathological damages caused by Delta are weaker than that caused by Alpha, while the variant Beta caused the most severe outcomes among the three VOCs (Figure 3B,C). In comparison, Alpha and MASCp6 infection caused comparable pathological damages, while the pathological damages caused by Beta were slightly weaker than that caused by MASCp36 (Figure 3B,C). As shown in Figure 3C, the severity of lung injury induced by VOCs and mouse-adapted strains is consistent with their infectivity in the lower respiratory tract.

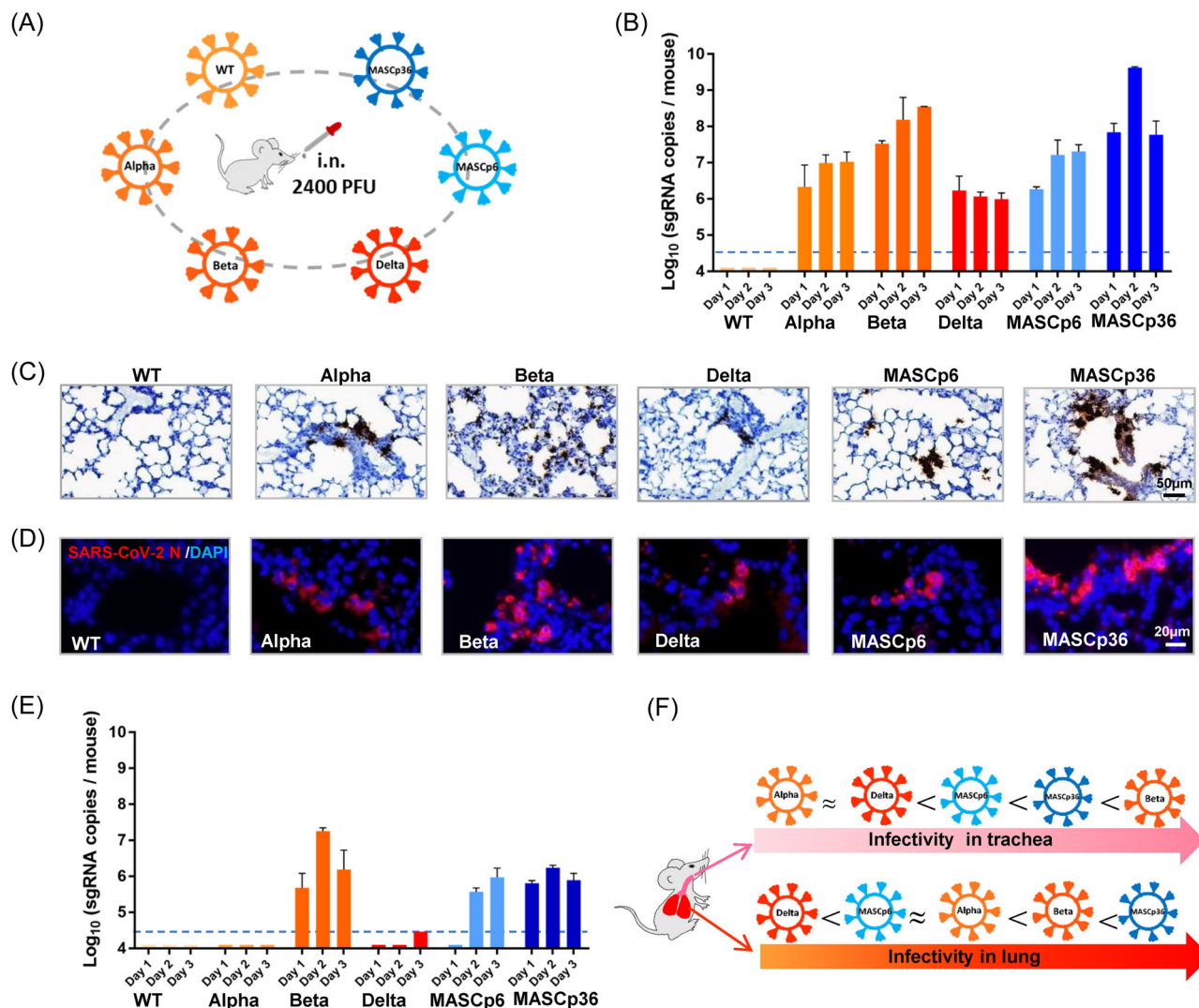


FIGURE 2 Intranasal infection of SARS-CoV-2 variants or mouse-adapted SARS-CoV-2 in laboratory standard mice. (A) Nine-month-old female BALB/c mice were intranasally infected with 2.4×10^3 PFU of WT, Alpha, Beta, Delta, MASCP6 or MASCP36, and the infected mice were killed on indicated time points for tissue collection. (B) SARS-CoV-2 sgRNA loads in lung tissues of infected mice. Each tissue was subjected to viral sgRNA copy analysis by RT-qPCR. The dotted lines denote the detection limit ($n = 3$). (C) ISH assay for viral RNA in lung tissues from infected mice on Day 3 post-infection. Positive signals are shown in brown. (D) Immunofluorescence staining of mouse lung paraffin sections for SARS-CoV-2 N protein (green) and 4,6-diamino-2-phenyl indole (blue). (E) SARS-CoV-2 sgRNA loads in the trachea of infected mice. Each tissue was subjected to viral sgRNA copy analysis by RT-qPCR. The dotted lines denote the detection limit ($n = 3$). (F) The rank of the infectivity of VOCs and mouse-adapted strains in trachea or lung of mice

3.4 | Inflammatory response by intranasal infection of VOCs in mice

To investigate the inflammatory response induced by VOCs, Luminex cytokine analysis for the lung homogenates harvested from mice on Day 2 post-infection was performed. Results showed that only 3 out of 36 detected cytokines were significantly elevated in comparison with the mock, including IL-10, G-CSF, and M-CSF (Figure 4A,B). In comparison, 18 cytokines were elevated to higher levels in Alpha-infected mice (Figures 4A and S1). As we expected, the Beta induced the strongest inflammatory response among the three VOCs: 33 out of the 36 detected cytokines were

obviously elevated, and more than 20 cytokines were elevated more than 10 times (Figure 4A). These results indicate that Delta infection can only induce a slight inflammatory response, which is much weaker than that induced by the variant Alpha, while the Beta variant is able to induce the strongest inflammatory response among the three VOCs. It seems that the inflammatory response induced by these variants is positively associated with the virus replication in the lungs of infected mice. However, interestingly, Alpha infection elevated higher levels of cytokine production in comparison with MASCP6 (Figures 4A and S1), despite they produced similar levels of sgRNA in the lung tissues as mentioned above (Figure 2A), indicating that viral replication

(A)

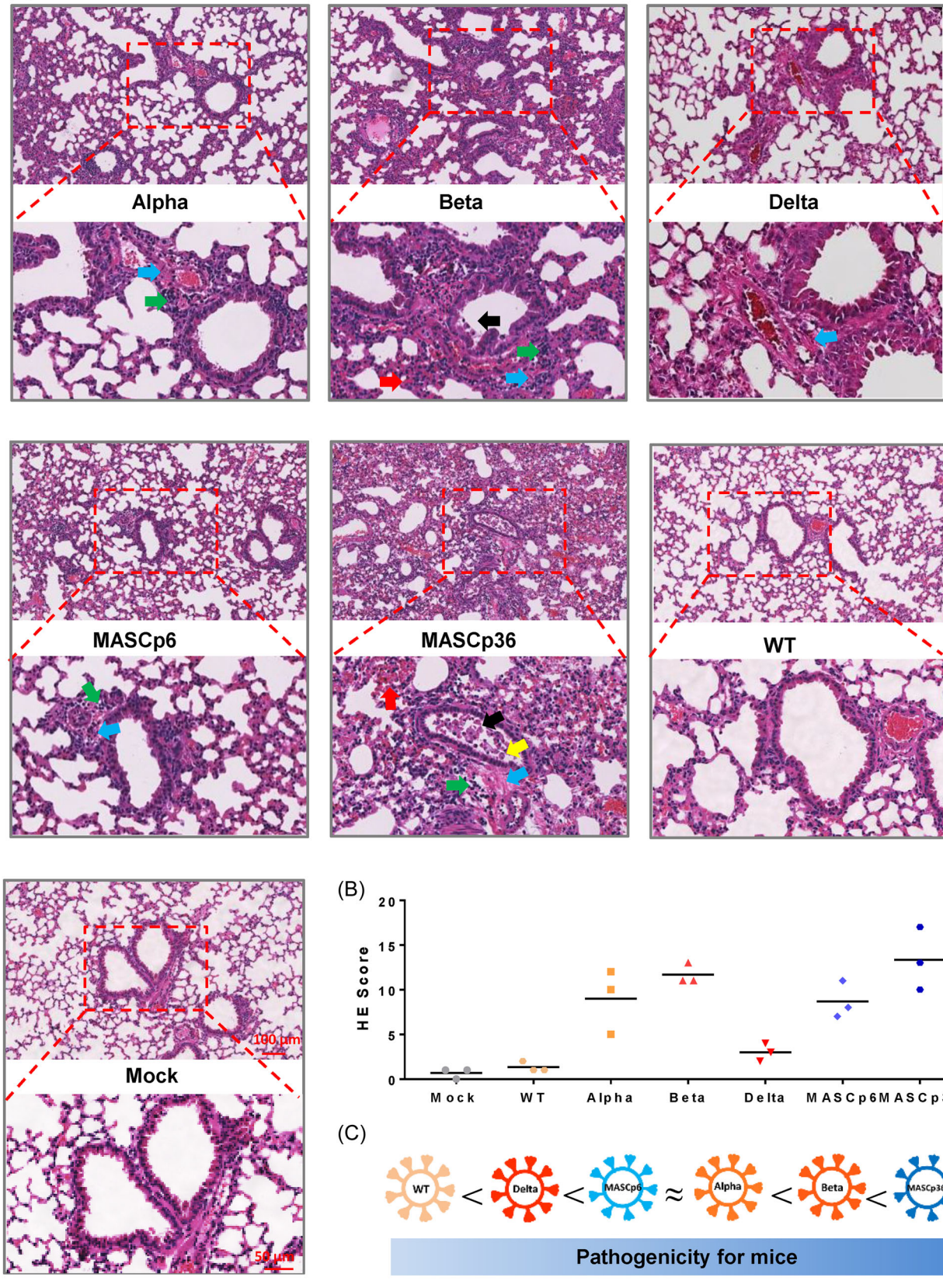


FIGURE 3 (See caption on next page)

may not be the only determinant for SARS-CoV-2-elevated inflammatory response.

4 | DISCUSSION

SARS-CoV-2 variants, especially the VOCs, have caused great concerns of immune escape and enhanced transmission in human populations.^{11,21-26} What's worse, more and more amino acid

mutations that occurred in these variants were demonstrated to have the potential of expanding its host range.¹⁰⁻¹³ Among these, the mutations having the potential of increasing the infectivity in mice are especially focused because of the wide distribution of this species around humans. As we concluded in Figure S2, 16 mutations in S protein have been confirmed to have the potential of increasing infectivity in mice.¹⁰⁻¹³ However, until now, only the SARS-CoV-2 variant Beta has been confirmed to be able to infect mice. Whether other variants, especially the newly emerged variant Delta carrying

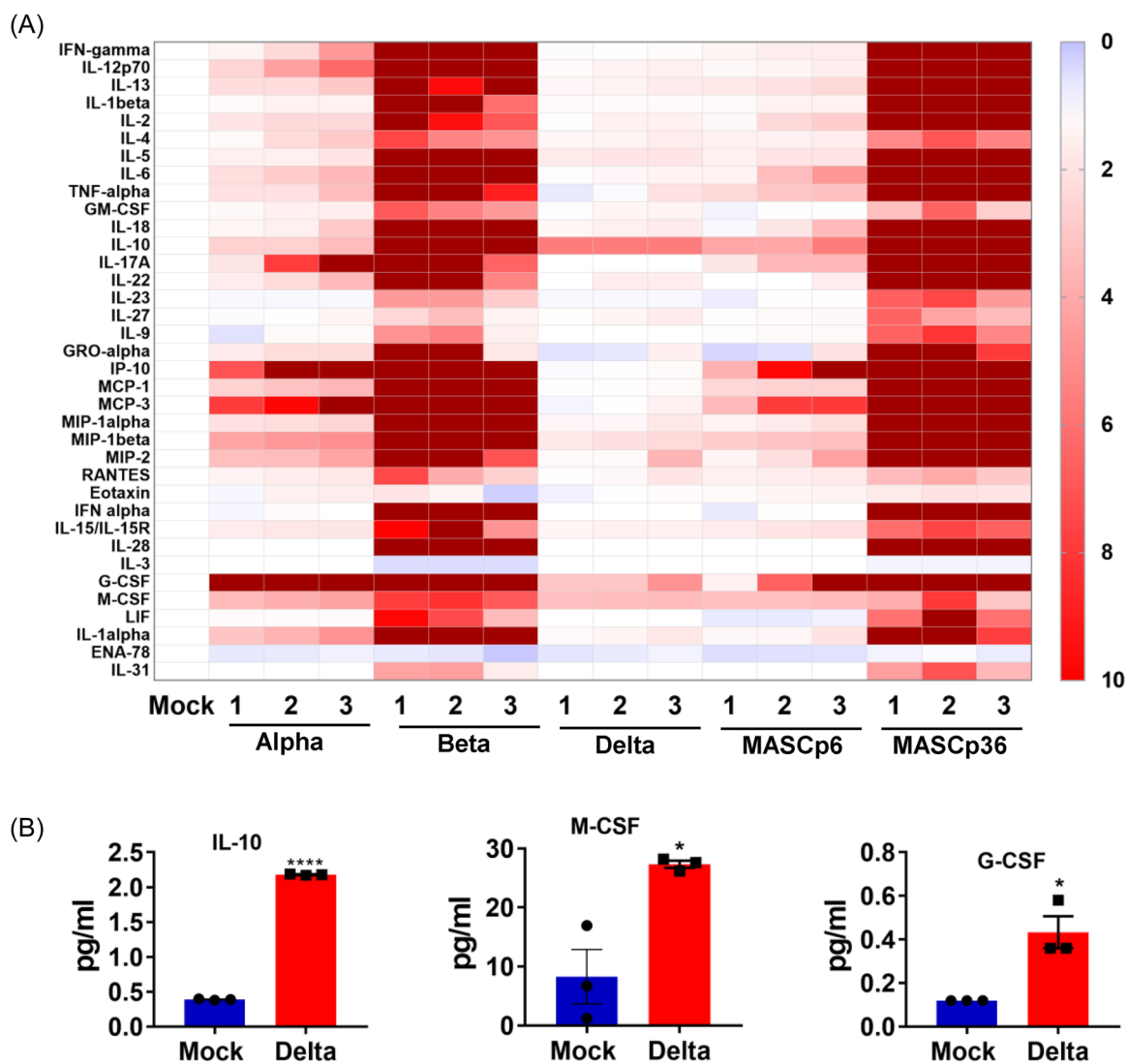


FIGURE 4 Inflammatory response in laboratory standard mice infected with SARS-CoV-2 variants or mouse-adapted SARS-CoV-2. (A) Relative cytokine production in lung homogenates of infected mice on Day 2 post-infection to the mock (PBS). (B) Representative cytokines are significantly elevated by data infection. Samples outside the defined range were indicated by dull red. * $p < 0.05$; **** $p < 0.0001$

FIGURE 3 Pathological changes in laboratory standard mice infected with SARS-CoV-2 variants or mouse-adapted strains. (A) Hematoxylin and eosin (H&E) staining of lung tissue sections from mice infected mice on Day 3 post-infection or mock. Inflammatory cell infiltration (green arrow), edema around vessels (blue arrow), hemorrhage (red arrow), desquamative epithelial cells (black arrow), and macrophages (yellow arrow) in bronchiole tubes are indicated. (B) Semiquantitative analysis of the H&E-stained lung sections. (C) Score ranking for the pathogenicity of SARS-CoV-2 variants and mouse-adapted strains.

completely different mutations in the RBD from previous variants, have obtained the infectivity in mice, worth being further investigated. Thus, in this study, we adopted three VOCs, Alpha, Beta, and Delta, to systematically investigate their infectivity and pathogenicity for mice, and confirmed that all three VOCs are able to infect laboratory standard mice and cause pulmonary pathology, highlighting the ongoing risk of spillover from human to mice during the continued evolution of SARS-CoV-2.

By our study, it was found that the variant Alpha can effectively infect mice, and the infectivity is comparable with MASCP6. In our previous study, it has been demonstrated that the mutation N501Y can effectively enhance the binding affinity of the RBD to mACE2, and play a key role in the infectivity of the mouse-adapted strain MASCP6 in mice. As the Alpha and MASCP6 carry the same mutation N501Y in the RBD and no other mutations are found in the S protein of MASCP6 outside of the RBD, we can learn that the mutation N501Y may also be the main determinant for the infectivity of Alpha in mice. Despite the 69–70 deletions outside of the RBD within Alpha S protein were demonstrated to be able to slightly increase the infectivity of SARS-CoV-2 pseudoviruses in mACE2-expressing cells, it seems that they did not play an important role in the infectivity of Alpha *in vivo*, as the Alpha did not show higher replication capability in lung tissues compared with MASCP6. In the RBD of Beta, another two mutations K417N and E484K are found, which have been confirmed to be able to increase the binding affinity of RBD to mACE2 in addition to N501Y. Thus, the additional mutations, K417N and E484K, may contribute to the increased infectivity of the Beta in mice in comparison with the Alpha.

Despite the RBD of Delta having a lower binding affinity to mACE2 than the RBD of Alpha or Beta carrying the mutation N501Y, it still enables the variant to infect mice. Before our study, several studies demonstrated that the capability of the mutations L452R/T478K to increase the infectivity of the SARS-CoV-2 pseudoviruses in mACE2-expressing cells was not as high as the mutation N501Y.^{12,13} Despite that, our study with the variant Delta *in vivo* clearly confirmed that the variant Delta still obtained the capability to infect mice, despite the infectivity being lower than the variants carrying the mutation N501Y. A recent study showed that no viral sgRNA was detected in Delta-infected C57/BL6 mice.²⁷ By comparison, we found that we adopted aged BALB/c mice (9-month-old) for challenging, whereas young C57/BL6 mice (8-week-old) were chosen in the previous study. Recently, it has been confirmed that the mouse-adapted strain was more virulent to BALB/c mice compared with the C57/BL6 mice, and more virulent to aged mice compared with the young ones.^{9,17,19} Thus, the difference in mouse strain and age may be why no Delta sgRNA was detected in the previous study.

In consideration of the time-sequence of these three VOCs appeared, the infectivity for mice acquired by SARS-CoV-2 during its evolution in humans showed a first increased and then decreased trend. Despite the infectivity for mice did not keep increasing, the acquisition of infectivity for mice by all three VOCs indicates that the risk of SARS-CoV-2 spillover from humans to mice may not be a transient accident. In fact, more and more mutations are confirmed

to be able to render SARS-CoV-2 to infect mice, such as the newly emerged L452R and T478K in Delta, making the spillover risk more unpredictable and uncontrollable. Thus, the newly emerged variants shall be continuously monitored for their cross-species infectivity, and the related mutations in S protein, especially those in the RBD, are worth being further identified. Interestingly, by our study, it was confirmed that the mouse infectivity is comparable between the VOCs and mouse-adapted strains sharing key mutations in the RBD, indicating the key amino acid mutations in the RBD of mouse-adapted strains may be referenced as an early-warning indicator for predicting the spillover risk of newly emerging SARS-CoV-2 variants, which may be helpful for easing the difficulty of monitoring measures mentioned above. In fact, another VOC, the Omicron, appeared after we have just finished this study. Despite we did not include this variant in this study, we made an alignment between the S genes of Omicron and mouse-adapted strains, and surprisingly found that all six amino acid mutation sites in the S gene of mouse-adapted strains (K417, Q493, Q498, N501, H655, and N969) also occurred in Omicron variant (Figure S3), and three of them are the same (K417N, N501Y, and H655Y), indicating the Omicron variant also have great potential to infect mice.

In this study, we adopted two mouse-adapted strains for infectivity and pathogenicity in comparison with VOCs, and found that the variant Alpha and mouse-adapted strain MASCP6 show comparable infectivity in lung tissues of infected mice, but Alpha induces a stronger inflammatory response. A recent study showed that SARS-CoV-2 exacerbates pro-inflammatory responses in myeloid cells not only through the interaction between the RBD and Tweety family member 2, but also through the interaction between the C-type lectin receptors and N-terminal domain (NTD)/C-terminal domain (CTD) of the S protein.²⁸ As we observed above, MASCP6 and Alpha harbor the same mutation in RBD, and no amino acid mutations are found outside of RBD within the S protein of MASCP6, while there are several amino acid mutations or deletions in the NTD and CTD of the Alpha S protein. Hence, these additional mutations or deletions may contribute to the stronger inflammatory response induced by Alpha by affecting the interaction between the NTD/CTD and the C-type lectin receptors, indicating that the mutations outside of the RBD should not be neglected during further surveillance.

By comparison, another notable finding is that the tropism of the VOCs and mouse-adapted strains for the upper respiratory tract is not always positively associated with that for the lower respiratory tract. As we observed in this study, Alpha and MASCP6 showed similar infectivity in lung tissues, but MASCP6 showed higher infectivity in the trachea; Beta showed slightly lower infectivity in lung tissues but higher infectivity in the trachea when compared with MASCP6. This phenomenon indicates that SARS-CoV-2 may change its tropism for the upper or lower respiratory tract during its evolution, which is in accordance with recent findings that the virus distribution in the respiratory tracts is obviously different between COVID-19 patients infected with recently emerged SARS-CoV-2 variants and prototype SARS-CoV-2.²⁹ Thus, our study may also

provide a platform for investigating the mechanism of the tropism change of the newly emerged variants.

5 | CONCLUSION

Our results confirmed that the spillover risk of SARS-CoV-2 from humans to mice may persistently exist during the continued evolution of SARS-CoV-2 in humans, indicating the monitoring and preventive measures for cross-species infection of emerging SARS-CoV-2 variants should be constantly implemented. Meanwhile, our results also provided a reference for taking the key amino acid mutations in the RBD of mouse-adapted strains as an early-warning indicator for predicting the spillover risk of newly emerging SARS-CoV-2 variants.

AUTHOR CONTRIBUTIONS

Cheng-Feng Qin and Qi Chen conceived and designed the project. Qi Chen, Xing-Yao Huang, Yu Liu, Meng-Xu Sun, Chao Zhou, Dan Luo, and Rong-Rong Zhang performed the experiments. Qi Chen, Bin Ji, Hang Chi, Ying Tian, and Xiao-Feng Li analyzed the data. Cheng-Feng Qin and Qi Chen wrote and finalized the manuscript. All authors read and approved the manuscript.

ACKNOWLEDGMENTS

This study was supported by the National Key Research and Development Projects of the Ministry of Science and Technology of China (2021YFC2301300), the National Key Research and Development Project of China (2020YFC0842200, 2020YFA0707801, and 2021YFC0863300), and the National Natural Science Foundation of China (No. 82041044). C.-F.Q. was supported by the National Science Fund for Distinguished Young Scholars (81925025), the Innovative Research Group (81621005) from the NSFC, and the Innovation Fund for Medical Sciences (2019-I2M-5-049) from the Chinese Academy of Medical Sciences.

CONFLICTS OF INTEREST

The authors declare no conflicts of interest.

DATA AVAILABILITY STATEMENT

The data supporting the findings of the current study are available from the corresponding author upon reasonable request.

ORCID

Cheng-Feng Qin  <http://orcid.org/0000-0002-0632-2807>

REFERENCES

- Singh J, Rahman SA, Ehtesham NZ, Hira S, Hasnain SE. SARS-CoV-2 variants of concern are emerging in India. *Nat Med*. 2021;27(7):1131-1133.
- Tao K, Tzou PL, Nouhin J, et al. The biological and clinical significance of emerging SARS-CoV-2 variants. *Nat Rev Genet*. 2021;22(12):757-773.
- Davies NG, Abbott S, Barnard RC, et al. Estimated transmissibility and impact of SARS-CoV-2 lineage B.1.1.7 in England. *Science*. 2021;372:6538.
- Tegally H, Wilkinson E, Giovanetti M, et al. Detection of a SARS-CoV-2 variant of concern in South Africa. *Nature*. 2021;592(7854):438-443.
- Chen Q, Huang XY, Sun MX, et al. Transient acquisition of cross-species infectivity during the evolution of SARS-CoV-2. *Natl Sci Rev*. 2021;8(11):nwab167.
- Choi JY, Smith DM. SARS-CoV-2 variants of concern. *Yonsei Med J*. 2021;62(11):961-968.
- Zhou P, Yang XL, Wang XG, et al. A pneumonia outbreak associated with a new coronavirus of probable bat origin. *Nature*. 2020;579(7798):270-273.
- Letko M, Marzi A, Munster V. Functional assessment of cell entry and receptor usage for SARS-CoV-2 and other lineage B betacoronaviruses. *Nat Microbiol*. 2020;5(4):562-569.
- Sun S, Gu H, Cao L, et al. Characterization and structural basis of a lethal mouse-adapted SARS-CoV-2. *Nat Commun*. 2021;12(1):5654.
- Li Q, Nie J, Wu J, et al. SARS-CoV-2 501Y.V2 variants lack higher infectivity but do have immune escape. *Cell*. 2021;184(9):2362-2371.e9.
- Wang R, Zhang Q, Ge J, et al. Analysis of SARS-CoV-2 variant mutations reveals neutralization escape mechanisms and the ability to use ACE2 receptors from additional species. *Immunity*. 2021;54(7):1611-1621.e5.
- Zhang L, Cui Z, Li Q, et al. Ten emerging SARS-CoV-2 spike variants exhibit variable infectivity, animal tropism, and antibody neutralization. *Commun Biol*. 2021;4(1):1196.
- Ren W, Ju X, Gong M, et al. Characterization of SARS-CoV-2 variants B.1.617.1 (Kappa), B.1.617.2 (Delta) and B.1.618 on cell entry, host range, and sensitivity to convalescent plasma and ACE2 decoy receptor. *bioRxiv*. 2021;2021.09.03.458829
- Gu H, Chen Q, Yang G, et al. Adaptation of SARS-CoV-2 in BALB/c mice for testing vaccine efficacy. *Science*. 2020;369(6511):1603-1607.
- Zhang Y, Huang K, Wang T, et al. SARS-CoV-2 rapidly adapts in aged BALB/c mice and induces typical pneumonia. *J Virol*. 2021;95(11):e02477-20.
- Muruato A, Vu MN, Johnson BA, et al. Mouse-adapted SARS-CoV-2 protects animals from lethal SARS-CoV challenge. *PLoS Biol*. 2021;19(11):e3001284.
- Wang J, Shuai L, Wang C, et al. Mouse-adapted SARS-CoV-2 replicates efficiently in the upper and lower respiratory tract of BALB/c and C57BL/6J mice. *Protein Cell*. 2020;11(10):776-782.
- Leist SR, Dinnon KH, 3rd, Schäfer A, et al. A mouse-adapted SARS-CoV-2 induces acute lung injury and mortality in standard laboratory mice. *Cell*. 2020;183(4):1070-1085.e12.
- Dinnon KH, 3rd, Leist SR, Schäfer A, et al. A mouse-adapted model of SARS-CoV-2 to test COVID-19 countermeasures. *Nature*. 2020;586(7830):560-566.
- Chen Q, Huang XY, Tian Y, et al. The infection and pathogenicity of SARS-CoV-2 variant B.1.351 in hACE2 mice. *Virol Sin*. 2021;36(5):1232-1235.
- Li M, Lou F, Fan H. SARS-CoV-2 variants of concern delta: a great challenge to prevention and control of COVID-19. *Signal Transduct Target Ther*. 2021;6(1):349.
- Hoffmann M, Arora P, Groß R, et al. SARS-CoV-2 variants B.1.351 and P.1 escape from neutralizing antibodies. *Cell*. 2021;184(9):2384-2393.e12.
- Harvey WT, Carabelli AM, Jackson B, et al. SARS-CoV-2 variants, spike mutations and immune escape. *Nat Rev Microbiol*. 2021;19(7):409-424.

24. Garcia-Beltran WF, Lam EC, St, St. Denis K, et al. Multiple SARS-CoV-2 variants escape neutralization by vaccine-induced humoral immunity. *Cell*. 2021;184(9):2372-2383.e9.
25. Deng X, Garcia-Knight MA, Khalid MM, et al. Transmission, infectivity, and neutralization of a spike L452R SARS-CoV-2 variant. *Cell*. 2021;184(13):3426-3437.e8.
26. Cai Y, Zhang J, Xiao T, et al. Structural basis for enhanced infectivity and immune evasion of SARS-CoV-2 variants. *Science*. 2021;373(6555):642-648.
27. Shuai H, Chan JF, Yuen TT, et al. Emerging SARS-CoV-2 variants expand species tropism to murines. *EBioMedicine*. 2021;73:103643.
28. Lu Q, Liu J, Zhao S, et al. SARS-CoV-2 exacerbates proinflammatory responses in myeloid cells through C-type lectin receptors and Tweety family member 2. *Immunity*. 2021;54(6):1304-1319.e9.
29. Luo CH, Morris CP, Sachithanandham J, et al. Infection with the SARS-CoV-2 delta variant is associated with higher infectious virus

loads compared to the alpha variant in both unvaccinated and vaccinated individuals. *medRxiv*. 2021;20.

SUPPORTING INFORMATION

Additional supporting information can be found online in the Supporting Information section at the end of this article.

How to cite this article: Chen Q, Huang X-Y, Liu Y, et al. Comparative characterization of SARS-CoV-2 variants of concern and mouse-adapted strains in mice. *J Med Virol*. 2022;94:3223-3232. doi:10.1002/jmv.27735